An experimental study of the coalescence between a drop and an interface in Newtonian and polymeric liquids

Xiaopeng ChenShreyas MandreJames J. Feng

Articles you may be interested in

Partial coalescence between a drop and a liquid-liquid interface
Physics of Fluids **18**, 051705 (2006); 10.1063/1.2201470

Drop coalescence through planar surfaces
Physics of Fluids **18**, 072105 (2006); 10.1063/1.2227435

The influence of surface tension gradients on drop coalescence
Physics of Fluids **21**, 072107 (2009); 10.1063/1.3177339

A computational study of the coalescence between a drop and an interface in Newtonian and viscoelastic fluids
Physics of Fluids **18**, 102102 (2006); 10.1063/1.2364144

Drop coalescence through a liquid/liquid interface
Physics of Fluids **16**, 2170 (2004); 10.1063/1.1735686

The coalescence cascade of a drop
Physics of Fluids **12**, 1265 (2000); 10.1063/1.870380

An experimental study of the coalescence between a drop and an interface in Newtonian and polymeric liquids

Xiaopeng Chen
*Department of Chemical and Biological Engineering, University of British Columbia,
Vancouver, British Columbia V6T 1Z3, Canada*

Shreyas Mandre
Department of Mathematics, University of British Columbia, Vancouver, British Columbia V6T 1Z2, Canada

James J. Feng[a)]
*Departments of Chemical and Biological Engineering and Mathematics, University of British Columbia,
Vancouver, British Columbia V6T 1Z3, Canada*

When a water drop falls onto an oil-water interface, the drop usually rests for some time before merging with the water underneath the interface. We report experiments on this process using water- and oil-based Newtonian liquids and polymer solutions, with an emphasis on the non-Newtonian effects. We deduce that the drop surface is immobilized by contaminants pre-existing in the fluids, and find that the rest time scales with the matrix viscosity for Newtonian fluids. The results are compared with lubrication models for film drainage. If the surrounding matrix is a dilute polymer solution, the rest time is identical to that for a matrix of the solvent alone. Further investigation indicates that the polymer molecules have been cleared from the film by surface adsorption. Depending on the fluid properties and drop size, the drop-interface merging may be completed in one shot or through a cascade of partial coalescence. Partial coalescence occurs for an intermediate range of drop sizes; it is arrested by viscosity for smaller drops and by gravity for larger ones. When either the drop or the matrix phase is a polymer solution, viscoelasticity is shown to suppress partial coalescence for smaller drops. This is apparently due to the inhibition of capillary pinch-off which would otherwise produce a secondary drop before the merging is complete. © *2006 American Institute of Physics*. [DOI: 10.1063/1.2349586]

I. INTRODUCTION

Consider an interface between two immiscible fluids: fluid A being lighter and resting on top of fluid B. When a drop of fluid B is released in fluid A, it settles onto the interface. Let us confine ourselves to relatively low settling speeds so as to exclude violent impacts. Two interesting phenomena ensue: first the drop rests on the interface for an extended time, and then it coalesces with the interface. These seemingly mundane processes in fact reveal a rich range of fluid physics and offer a unique opportunity to investigate the interfacial dynamics between immiscible fluids. Hereafter, we will refer to fluid A as the matrix phase, and fluid B as the drop phase even though it also occurs in the lower bulk.

As the drop approaches the interface, the matrix fluid beneath the drop is squeezed out and forms a thin film. Further drainage of the film is governed largely by the balance between gravity, which produces a high pressure in the center of the film, and viscous force resisting flow in the thin film. Thus, the drainage becomes slower as the film thins, and lubrication models indicate that the film thickness will not shrink to zero in finite time.[1] In reality, short-range non-hydrodynamic forces, such as van der Waals attraction between the drop surface and the interface below it, become important when the film gets thin enough. The film thus becomes unstable and ruptures at some point that is not necessarily the center of the film.

After the film ruptures, the point of contact between the two interfaces rapidly enlarges, under the action of interfacial tension, into an opening through which the drop fluid dumps into the lower bulk. This deflation of the drop is driven by interfacial tension and gravity. Under certain conditions, the merging does not proceed to completion at once. Instead, a "partial coalescence" occurs when the liquid column connecting the drop to the lower bulk forms a neck and pinches off, leaving a daughter drop on the interface. The process of film drainage starts anew, and the episode may repeat itself up to eight times before the drop finally merges into the bulk.

The drop-interface coalescence process has attracted the attention of fluid dynamicists and engineers since the early 1960s.[1,2] Film drainage received most of the attention because experimentally it is relatively straightforward to measure the evolution of the film thickness and the rest time, and theoretically the process lends itself well to lubrication analysis. Numerical simulations have been conducted as well.[3,4] Charles and Mason[1] showed that the rest time, the interval between a suitably defined start of film drainage and the final rupture, exhibits a Gaussian-type distribution, and that its mean value t_R varies with the drop diameter D as

---

[a)]Author to whom correspondence should be addressed. Electronic mail: jfeng@chml.ubc.ca

$D^{3.15}$. They also devised a simple model that treats the thinning of the film as that between two solid disks being squeezed together. This predicts a scaling of $t_R \sim D^5$. Since then, numerous more elaborate models have been constructed, brief reviews of which can be found in the literature.[5–8] These are subject to various assumptions on whether the film has a uniform thickness or a profile featuring a dimple,[9] whether the interfaces are immobilized by viscosity or surfactants,[7,10,11] whether van der Waals forces are important,[5,12] and whether the rupture is ultimately due to drainage or some form of film instability.[5,13] Owing to such complicating factors, experimental data from different groups are often inconsistent, and it is difficult to say which model is the most satisfactory. Certainly none has offered unequivocal quantitative agreement with data obtained in clearly characterized experiments.

Partial coalescence, in contrast, has received only a handful of experimental studies[13–16] since the pioneering work of Charles and Mason,[2] and few theoretical analysis. Charles and Mason ascribed the pinch-off of the secondary drop to capillary instability. Upon film rupture, a ring-shaped capillary wave travels up the mother drop and transforms it into a liquid column. With continued drainage, the column shrinks in diameter, but not in height, until it is thin enough to sustain Rayleigh instability. Based on this picture, the daughter drop size should be proportional to the dominant wavelength on the column. The latter in turn depends on the column's height, which is roughly equal to the diameter of the mother drop. This leads to the prediction that the size ratio between the daughter drop and the mother drop should be a constant. This seems to be the case under some conditions,[2] while under others, the size ratio tends to decrease as the mother drop gets smaller.[12]

More recently, Thoroddsen and Takehara[14] demonstrated that the partial coalescence cascade is self-similar in a range of parameters where both gravity and viscosity are unimportant. This is most clearly seen by considering the four governing dimensionless groups of the system: the Ohnesorge number Oh, the Bond number Bo, and the density and viscosity ratios between the drop and matrix phases:

$$Oh = \frac{\mu_1}{(\bar{\rho}\sigma D)^{1/2}}, \tag{1}$$

$$Bo = \frac{\Delta\rho g D^2}{\sigma}, \tag{2}$$

$$\rho_* = \frac{\rho_1}{\rho_2}, \tag{3}$$

$$\mu_* = \frac{\mu_1}{\mu_2}, \tag{4}$$

where subscripts 1 and 2 denote, respectively, the drop and matrix phases, $\bar{\rho} = (\rho_1 + \rho_2)/2$, $\Delta\rho = \rho_1 - \rho_2$, g is the gravitational acceleration and σ is the interfacial tension. If the viscosities are low, there exists an intermediate range of drop diameter in which Bo and Oh are both vanishingly small, and the dynamics is governed entirely by capillarity and inertia.

Then the size ratio ζ depends only on ρ_* and μ_*, and remains a constant through the successive cycles of partial coalescence.

Apparently Mohamed-Kassim and Longmire[15] made the only attempt so far at formulating a criterion for partial coalescence. Analyzing their own data, which show no partial coalescence, and those in the literature that do,[2,14] Mohamed-Kassim and Longmire suggested that partial coalescence occurs if Bo·Oh < 0.02 − 0.03. The Ohnesorge number Oh, computed using the averaged viscosity and density between the two components, signifies the tendency of viscosity in both phases to damp capillary waves and suppress partial coalescence. Bo, on the other hand, indicates the tendency of gravity to inhibit partial coalescence. Thus, these authors argued that gravity, surface tension and viscosity all play roles in partial coalescence.

Previous work on drop-interface coalescence concerns mostly Newtonian fluids. In fact, the only investigation of non-Newtonian effects on this process appears to be Dreher et al.[17] They reported that adding polymers to the matrix fluid tends to prolong the rest time of water drops, and attempted to explain this phenomenon by the activation of elongational stress in the matrix fluid. In general, non-Newtonian fluids are important to engineering applications that involve drop-drop and drop-interface interactions, such as emulsification and liquid-liquid extraction. From a fundamental standpoint, drop-interface coalescence incurs severe stretching and deformation of the fluid bulk and interfaces, and should bring out interesting viscoelastic effects. These considerations have motivated the experiments reported in this paper.

We investigate the drop-interface coalescence using both Newtonian fluids and viscoelastic polymer solutions, and the latter may be in either the drop or the matrix. We discuss the drop-resting and coalescence stages separately, and focus on how viscoelasticity in either phase modifies the rest time and the partial coalescence cascade. As a baseline, we have studied Newtonian oil-water systems first. The Newtonian experiments on partial coalescence have yielded new insights into the phenomenon, which have been reported in a recent Letter.[18] For completeness of the logical structure and for comparison with non-Newtonian results, we have included a brief subsection on partial coalescence in Newtonian fluids.

The rest of the paper is organized as follows: Sec. II describes the experimental methodology, including the setup, materials, procedure, and operational protocols. Detailed results are presented and analyzed in Secs. III and IV, devoted to the rest time and partial coalescence, respectively. Each section presents results for Newtonian and non-Newtonian fluids in turn. Conclusions are drawn in Sec. V.

II. EXPERIMENTAL METHODOLOGY

A. Facilities

The experimental setup is schematically shown in Fig. 1. The fluids are contained in a square glass box (1) of dimensions 10 cm × 10 cm × 10 cm. In the center of the box sits a beaker (2) 5 cm in diameter and 7.5 cm in height. The aqueous phase fills the beaker and overflows into the glass con-
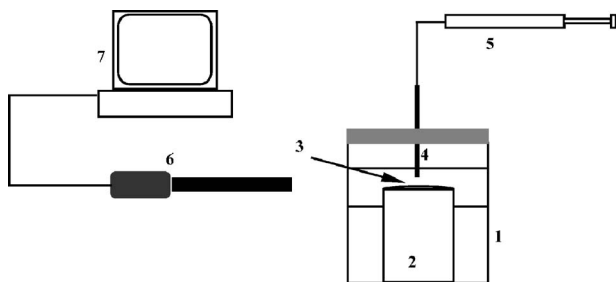
FIG. 1. Schematic of the experimental setup. 1: Container; 2: beaker; 3: liquid-liquid interface; 4: needle; 5: syringe; 6: camera; 7: computer.

tainer. Then the oil phase is added to the outer container. The interface formed on top of the beaker (3) is where coalescence takes place. The purpose of this setup is twofold: to renew and clean the interface by regularly overflowing the beaker, and to form a convex interface that is more easily observed and recorded by the camera (6) from the side. In a typical configuration, the layer of aqueous fluid in the glass box is 6 cm deep, and the oil layer on top of it is 3 cm thick. The upper surface of the oil layer is 1 cm below the Teflon lid that closes the container. A needle is installed on the lid, with its tip about 1.5 cm above the interface (3) on top of the beaker. Drops are released from the needle and settle onto the interface. The needle is connected to a syringe (5) through a Teflon tubing with a 0.71 mm inner diameter. Three types of needles have been used, with outer diameters of 0.74 mm, 0.82 mm, and 1.27 mm. For the two smaller needles, a threaded plunger syringe (No. 81242, Hamilton) is used for precise volume control; each revolution of the plunger outputs 5.29 μl of liquid. For the largest needle, a 1 ml glass syringe is used to generate larger drops with diameters up to 3 mm. The beaker is overflowed by a fine tube that goes through the lid into the beaker.

The two stages of the coalescence process to be studied, drop resting on the interface and partial coalescence, occur on two different time scales. The drop may sit on the interface for tens of seconds, while the partial coalescence occurs in only several milliseconds. The slow process is captured by a normal-speed CCD camera (WAT-902B, Watec) with a recording speed of 30 frames per second (fps), while the partial coalescence is recorded by a high speed camera (MS70K, Canadian Photonic Labs), with a speed up to 100 000 fps, depending on the area of image being captured. A zoom lens (4.5×, VZM 450i, Edmund) is attached to the camera (6) for a magnified view and better accuracy in measuring the drop size. The test cell is illuminated by a Schott cold light source (KL 2500 LCD). The video images are monitored and recorded by a Pentium-IV computer (7). In some cases, the lens-camera assembly is elevated and tilted at an angle up to 12° for a better view of the interface.

B. Materials

The drop and lower bulk phase is water-based while the matrix phase surrounding the drop is oil-based. Four types of solutions are used in this work:

- **Newtonian drop phase:** mixtures of water and glycerol (G33-4, Fisher Scientific) at various concentrations.
- **Viscoelastic drop phase:** solutions of polyethylene oxide (PEO, molecular weight $M_w \sim 0.6 - 1 \times 10^6$, PEO-3Z, Sumitomo Seika) in water.
- **Newtonian matrix phase:** mixtures of polybutene (PB, $M_w \sim 800$, INDOPOL H-35, BP Amoco) and decane.
- **Viscoelastic matrix phase:** solutions of polyisobutylene (PIB, $M_w \sim 2 \times 10^6$, Oppanol B 150, BASF) in decane and decane-PB mixtures.

All materials are used straight from the container with no further processing or refinement. The physical parameters of all liquids used are listed in Table I. A minor complication is that the experiments have involved two grades of decane. The first, from the Chemistry Store at UBC and of unknown purity, is the solvent in matrix fluids M1–M6, which are used in rest time measurements reported in Sec. III. The second, 99.9% pure from Fisher Scientific, occurs in fluids M7–M10 and were mostly used in the partial coalescence experiments of Sec. IV. The first kind has a lower interfacial tension with aqueous liquids than the second, and is probably of lower purity.

The viscosities are measured by a stress-controlled rheometer (C-VOR, Malvern) with a double-gap fixture (DG24/27 stainless steel). The densities are measured by a 10 ml specific gravity bottle (Fisher Scientific). The interfacial tension is measured by the ring method (Surface Tensiomat, Model 21, Cole-Parmer) and the pendant drop method.[19] Both methods are calibrated by measuring the surface tension of distilled water at room temperature, and the results agree closely with the standard value (72 dyn/cm at 20 °C).

The polymer solutions in Table I are dilute or semidilute, with concentrations close to the critical value c^* at which the polymer coils start to overlap in the solution.[20] The shear viscosity is essentially constant over a range of shear rate from 1 to 100 s^{-1}. Because of their diluteness, it is difficult to determine the relaxation time λ of the solutions using the ratio between normal and shear stresses or the loss and storage moduli. Instead, we measure the intrinsic viscosity of the solution $[\eta]_0$ and estimate λ from the longest Rouse time[21]

$$\lambda = \frac{6}{\pi^2} \frac{\eta_s [\eta]_0 M_w}{\mathcal{R}T}, \tag{5}$$

where η_s is the solvent viscosity, M_w is the molecular weight, $\mathcal{R}$ is the universal gas constant, and T is the absolute temperature. The relaxation time for solution D4 is comparable with the Zimm time[21] of a similar PEO solution calculated by Rodd *et al.*,[20] although the relaxation time measured by capillary breakup is several times longer. For M6, our λ is consistent with the observation of Dreher *et al.*[17] that strain-hardening onsets at a strain rate between 10^2 s^{-1} and 10^3 s^{-1} for a decane+20% PB+0.05% PIB solution. We did not measure the extensional viscosity of the polymer solutions, but expect significant increase of the Trouton ratio at high extensional rates.[17]

TABLE I. Physical properties of all the liquids used in this work. The interfacial tension values for the drop liquids are measured against decane (M7), and those for the matrix liquids are against water (D1). For liquid mixtures, the percentage given is volume fraction.

		Drop phase fluids			
Sol. No.	Composition	Density (g/ml)	Viscosity (mPa s)	Interfacial tension (dyn/cm)	Relaxation time (ms)
D1	water	1.00	1.0	45	⋯
D2	20% glycerol in water	1.06	2.1	37	⋯
D3	33% glycerol in water	1.10	3.4	32	⋯
D4	0.18 wt. % PEO in water	1.00	1.5	27	0.12
		Matrix phase fluids			
Sol. No.	Composition	Density (g/ml)	Viscosity (mPa s)	Interfacial tension (dyn/cm)	Relaxation time (ms)
M1	decane (UBC)	0.74	1.0	32	⋯
M2	20% PB in M1	0.77	2.0	26	⋯
M3	40% PB in M1	0.80	5.4	23	⋯
M4	0.5 wt. % PIB in M1	0.73	4.5	29	0.12
M5	0.77 wt. % PIB in M1	0.73	9.5	30	0.12
M6	0.5 wt. % PIB in M2	0.77	9.0	27	1.21
M7	decane (Fisher Sci.)	0.73	1.0	45	⋯
M8	20% PB in M7	0.76	2.0	30	⋯
M9	40% PB in M7	0.79	5.1	24	⋯
M10	0.5 wt. % PIB in M7	0.73	3.6	32	0.12

C. Procedure

It is well known that surface contaminants, such as adsorbed surfactants or dust particles, can greatly influence interfacial behavior, and they are difficult to avoid. Through trial and error, we have decided on a protocol for cleaning the experimental setup and filtering the liquids. By following the same procedure in all experiments, we keep the level of contaminants consistent and the outcome of the experiments reproducible.

Before every test, the lid, container and beaker are cleaned by detergent and then rinsed by tap water for about 1 min. Then they are rinsed 3–4 times in distilled water. The needle, tubing, and syringe are cleaned in the same way and then assembled. The aqueous solutions are prepared using distilled water. To remove particulate contaminants, all the solutions undergo microfiltration using a 0.2 μm pore-size syringe filter (RK-29550-08, Cole-Parmer). No further effort is made to remove surfactants that may be dissolved in the liquids. After feeding the liquids into the beaker and container, the container is sealed to avoid evaporation and contamination. The whole system is kept at room temperature for at least 10 h to ensure chemical equilibration before experiments.

During the experiment, the interface is cleaned and renewed after testing every 10 drops or so by overflowing the beaker with the aqueous solution (lower bulk and drop phase). Before each drop is released, it is hung from the tip of the needle for about 2 min for the interface to reach equilibrium. The size of the drop is measured through video images, with an error of 1 pixel corresponding to 3–20 μm depending on the magnification. Time is also measured from the captured footage, and the accuracy depends on the recording speed. At 8000 fps, for example, the moment of

daughter-drop pinch-off can be determined to within 62.5 μs. With normal recording speed of 30 fps, the rest times are accurate up to 16.7 ms.

III. EXPERIMENTAL RESULTS: REST TIME

A convenient quantity that characterizes the film drainage process is the rest time t_R, the interval between a suitably defined start of drainage and the point of film rupture. We report t_R measurements for Newtonian and polymeric liquids, and infer from them the roles played by fluid rheology, interfacial mobility, and surfactants.

A. Newtonian liquids

Most previous data on t_R were obtained for primary drops, namely those released directly from the needle. To achieve reproducible results, one must carefully control the specific conditions surrounding the release of the drop. For example, if the drop is released close to the interface and approaches it gradually, the start of film drainage is hard to pinpoint. At large Bond numbers, drop and interface deformation also adds to this uncertainty. If the fall is too rapid, on the other hand, the impact intrudes upon the process of film drainage. To minimize these complications, we have only measured the rest time of secondary and subsequent generations of drops in a cascade of partial coalescence. As a daughter drop falls toward the interface, there is a well-defined point when its velocity drops suddenly to zero. An example is shown in Fig. 2. We take this point to be the beginning of film drainage, and define t_R as the interval between this and the rupture of the film. Figure 3 demonstrates that secondary and later drops are immune to initial conditions that affect the primary one. The rest time, as a function
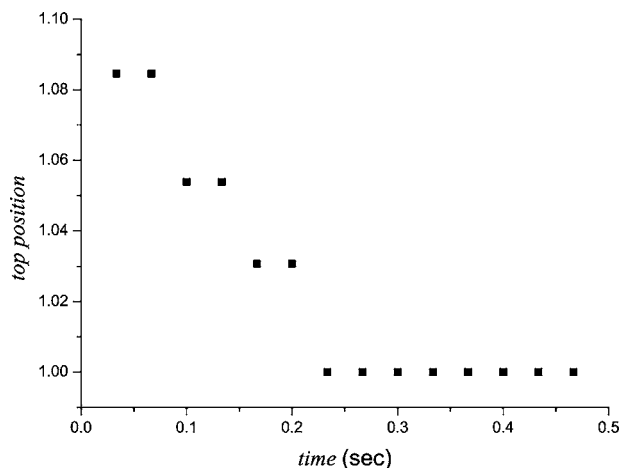
FIG. 2. The approach of a water drop to an interface between water (D1) and a decane-PB mixture (M3). The ordinate shows the position of the top of the drop measured from the interface, scaled by the drop diameter ($D \approx 0.26$ mm).

FIG. 4. Rest time for water drops on a decane-water interface: cumulative distribution for the rest time of drops of different size.

of the diminishing drop size through cycles of partial coalescence, is independent of the position and size of the needle from which the primary drop was released. The data also exhibit less scatter than for the primary drop, since the latter is subject to disturbances and variations in the drop release process. Similar tests were done on other liquid combinations with the same qualitative outcome. Another advantage of studying the daughter drops is that multiple data points for a series of drop sizes can be taken in one run.

As is well known, the rest time is stochastic and tends to assume a Gaussian-type distribution over a large number of measurements for the same system.[2,22] We have observed similar distributions; examples are shown in Fig. 4 for several sizes of water drops in decane (M1). Another random variable is the exact location of the rupture, which may be
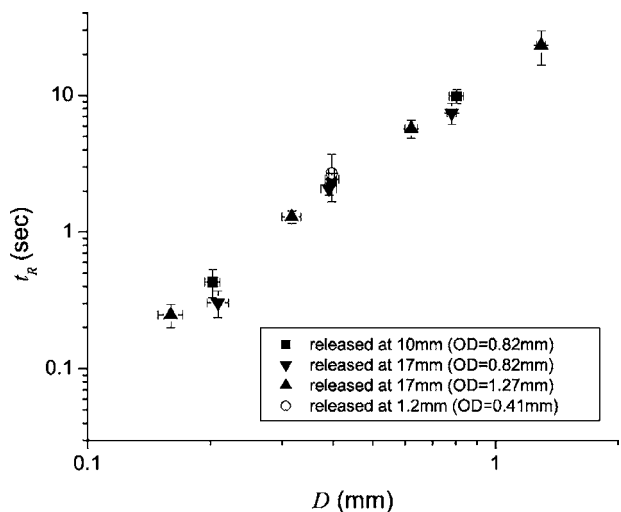

FIG. 3. Rest time for water drops on a decane (M1)-water interface: comparison of daughter drops generated from primary drops released from different heights above the interface and from needles of different sizes (OD). A single data point (open circle) for a primary drop is also shown for comparison.
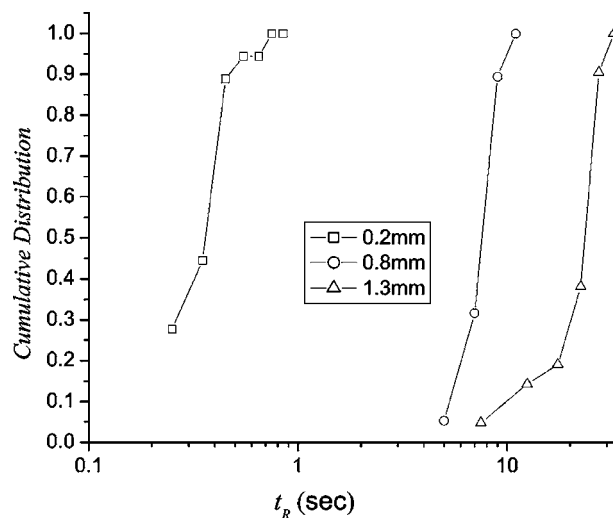
away from the axis of symmetry.[15] The stochasticity of film rupture originates from the nature of the disturbances that trigger the instability in the film after it has been thinned below a critical thickness. The t_R values reported in the rest of the paper are the mean of many measurements, and the standard deviations are indicated by error bars.

Before investigating the effects of fluid properties on t_R, the issue of interfacial mobility has to be clarified. The Appendix describes theoretical analysis and experiments that both show the drop interface to be completely immobilized for the fluids and drop size ranges in our study. Thus, circulation within the drop is suppressed and has no bearing on the film drainage process. We have focused, therefore, on varying the matrix properties by adding up to 40% of PB to decane (M1–M3), while keeping the drop phase the same (water). As shown in Table I, the density ρ_2, interfacial tension σ, and viscosity μ_2 of the matrix phase change by approximately 8%, 28%, and 440%, respectively.

Figure 5 shows the rest times measured for water drops in the three decane-based matrix fluids. One additional data set, for glycerol-water drops (D3) in a decane matrix, is also shown for comparison. Note first that changing the drop phase from pure water to water plus 33% glycerol has no effect on t_R, corroborating the prior conclusion that the drop surface is immobilized and the drop phase rheology does not affect the film drainage. Second, the rest time t_R becomes shorter as the drop diameter shrinks, and the relationship seems to obey a power law for all fluids tested. Third, t_R increases with the concentration of PB in the matrix. Since the matrix viscosity μ_2 is much more sensitive to the PB concentration than the interfacial tension σ and matrix density ρ_2 (Table I), the increase in t_R must be mostly due to the increase in μ_2. To develop a more precise relationship, we scale t_R by $\tau = D\mu_2/\sigma$, and the drop diameter D by the capillary length $D_g = \sqrt{\sigma/\Delta\rho g}$, and the data for all fluids seem to collapse onto a single curve in Fig. 5(b), which can be represented by a power law
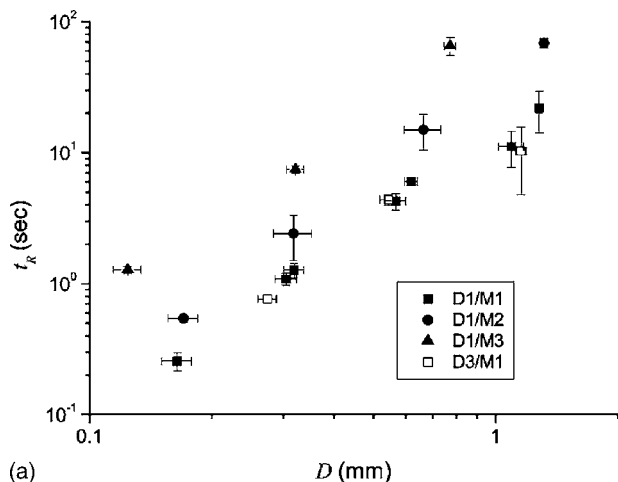
(a)
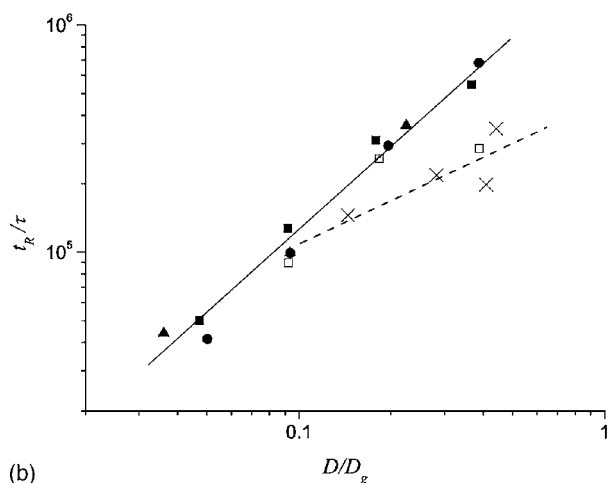
(b)

FIG. 5. Rest time t_R for water drops in a matrix of various concentrations of PB in decane. One set of data for drops of 33% glycerol in water (D3) in a decane matrix is also shown for comparison. (a) Dimensional rest time; (b) dimensionless rest time showing a power-law scaling with an index of 1.18. A data set from the literature (Ref. 23) (crosses) is also shown and seems to follow a power law with an index of 0.57.

$$\frac{t_R}{\tau} = 2.00 \times 10^6 \left(\frac{D}{D_g}\right)^{1.18}. \tag{6}$$

Previous experimental data from different groups show considerable variations. The discrepancies in t_R/τ range up to an order of magnitude,[1,5] and most data fall below ours. As an example, Fig. 5(b) plots a data set from Woods and Burrill[23] for drops of organic oils in water. The dimensionless rest time is shorter than ours and the increase with drop size is milder. A probable cause of such variations is surfactants intentionally added or naturally occurring as impurities in the fluids. For example, Woods and Burrill noted scatter in the data due to varying degrees of "interfacial aging." As we will discuss later, surface adsorption is believed to have affected t_R in our Newtonian (Fig. 6) and polymeric (Fig. 7) systems as well.

It is interesting to compare Eq. (6) to film drainage models in the literature. Because of interfacial immobilization and the importance of short-range forces,[8] we only consider
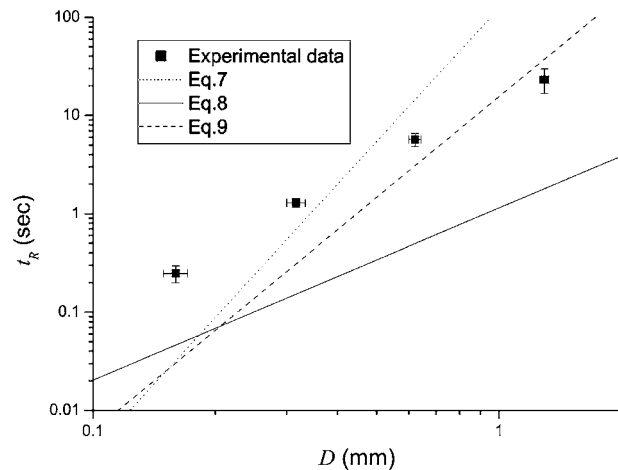

FIG. 6. Comparison of the measured rest time for the water-decane (D1/M1) system with predictions of three lubrication models.

models that have incorporated van der Waals forces and assumed zero slip on the drop surface. These include the parallel disk model of MacKay and Mason[12]

$$t_R = \frac{2\mu_2 R^{9/2} \Delta\rho g}{\sigma^{3/2} B^{1/2}}; \tag{7}$$

the cylinder model of Hodgson and Woods[10]

$$t_R = \frac{3\pi}{\sqrt{2}} \frac{\mu_2 R^{7/4}}{\sigma^{3/4} B^{1/4}}; \tag{8}$$

and the more sophisticated model of Chen et al.[5] that does not presume the interfacial geometry a priori

$$t_R = 2.4 \frac{\mu_2 R^{17/5} (\Delta\rho g)^{3/5}}{\sigma^{6/5} B^{2/5}}. \tag{9}$$

In these equations, $R = D/2$ is the drop radius and $B = 1 \times 10^{-28}$ J m is the Hamaker constant. The model predictions are compared with our data for the water-decane system in Fig. 6. All three models predict a power law $t_R \sim R^n$ with n
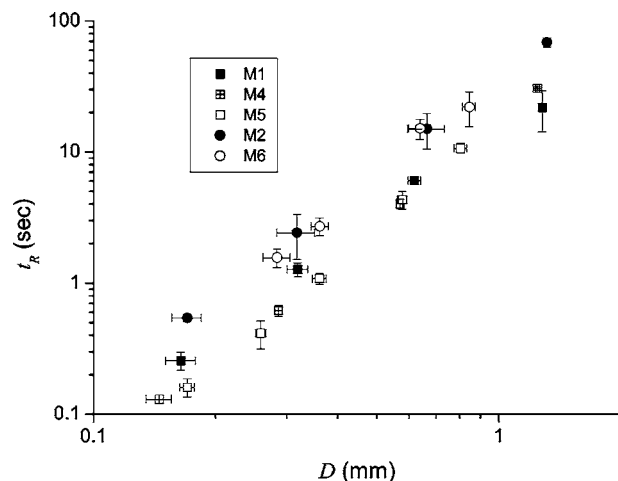

FIG. 7. Rest time t_R for water drops in polymeric matrices M4, M5, and M6. Data for two Newtonian matrices M1 and M2 are also shown for comparison.

ranging from 1.75 to 4.5, and our Eq. (6), with $t_R \sim R^{2.18}$, falls within this range. Chen *et al.*'s model is the most realistic of the three, and underpredicts our data by over an order of magnitude for small drops. With increasing drop size, the discrepancy diminishes and for the largest drop measured, there is close agreement between data and Eq. (9).

The discrepancy for small drops may be related to an intriguing idea regarding the role of surfactants in film rupture. Nikolov and Wasan[13] reported that without surfactants, t_R decreases with decreasing drop size, as is the case in our data. With added surfactants, however, t_R tends to increase for smaller drops. The authors argued that with surfactants, the film eventually thins down to a bilayer with no further drainage. Thus, t_R is dominated not by the drainage time but by the time taken for small holes to nucleate in the bilayer and destabilize it. The smaller the drop, the smaller the area of the film, and the lower the probability of film destabilization by nucleation. Hence the longer t_R. Ghosh and Juvekar[22] presented a similar model, although the rupture was ascribed to the diffusion of surfactants away from the edge of the film and the subsequent collapse of the bilayer. Although no surfactants have been added in our experiments, impurities in the form of dissolved surfactants almost certainly exist in the test fluids. A plausible scenario that accounts for the discrepancy in Fig. 6 is that such molecules have adsorbed onto the surface and hindered film rupture, especially for smaller drops. But in our case the surface concentration is probably far below full packing. A definite explanation requires systematic experiments with carefully controlled amounts of surfactants.

B. Non-Newtonian liquids

Since the drop-phase rheology is largely irrelevant to film drainage and rupture, we have examined the effects of adding polymers to the matrix phase only. The drop phase is pure water. Two Newtonian matrix fluids, M1 and M2 in Table I, are used as baselines against which the rest time for 3 viscoelastic matrix fluids M4, M5, and M6 are compared in Fig. 7. The data points fall into two groups; those liquids with decane as solvent (M1, M4, and M5) have produced approximately the same rest time t_R, while those with 20% PB in decane as solvent (M2 and M6) have a higher rest time. In other words, the presence of polymers has no effect on t_R; it scales with the solvent viscosity as for Newtonian liquids in the previous section.

With the interfaces immobilized, the flow in the draining film is mostly shear, and extension occurs at higher orders. This is because the radius of the film R_f is much larger than its thickness h. Typical values reported in the literature[10,12] are $h \sim 100$ nm and $R_f \sim 10$ μm. Mass balance dictates that the vertical velocity w and radial velocity u scale as

$$\frac{w}{u} \sim \frac{2\pi R_f h}{\pi R_f^2} = \frac{2h}{R_f} \ll 1. \tag{10}$$

Thus, the extension rate in squeezing the film w/h is much smaller than the shear rate u/h. If the interface slips, of course, the shear rate will be diminished and extension may become important. The radial velocity can be estimated from
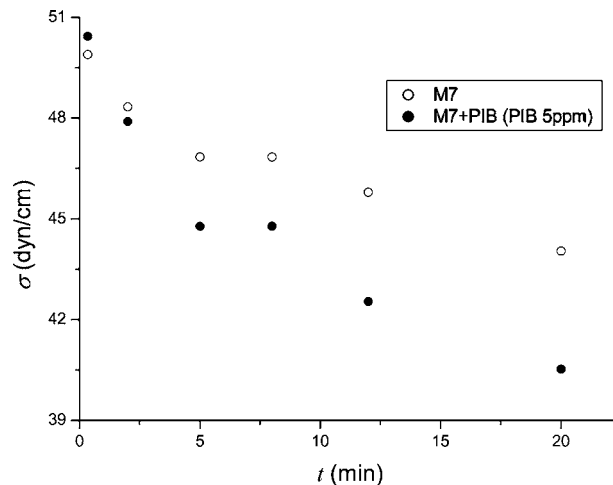

FIG. 8. Temporal evolution of the interfacial tension between water and the indicated liquid measured by the pendant drop method. The PIB concentration is roughly 5 ppm.

the volume of the film and the rest time $u \sim R_f/t_R \sim 10^{-3}$ cm/s if we take $R_f \sim 10$ μm and $t_R \sim 1$ s. The polymer relaxation time $\lambda \sim 1$ ms, and the Deborah number of the shear flow may be estimated as

$$\mathrm{De} = \frac{\lambda u}{h} \sim 0.1. \tag{11}$$

This is too low to activate viscoelastic effects such as shear-thinning or normal stress differences. Besides, the shear rheology of our polymeric liquids is simple, with a constant shear viscosity over a wide range of shear rate. Therefore, the polymer solutions in Fig. 7 are expected to behave as Newtonian fluids with an elevated shear viscosity (cf. Table I). The mystery is that they behave as Newtonian fluids with the *solvent* viscosity.

The coincidence of t_R with and without polymer in the matrix suggests that the polymer molecules have been depleted from the film. The most plausible mechanism for such depletion seems to be adsorption of the polymer molecules onto the interface, a process widely studied in the literature.[22,24–27] In general, polymers may adsorb onto interfaces through an array of potential mechanisms such as hydrogen bonding, attraction between charged groups and dispersion forces.[27] Although theoretical models exist, a quantitative estimation of the adsorption rate in our experiment would be difficult because many of the molecular properties are not known. Instead, we will present data and arguments that suggest: (a) the polymers in the matrix phase do adsorb onto the interface; (b) the rest time t_R is long enough for the adsorption to complete; and (c) the interface can accommodate all the polymer chains in these low-concentration solutions.

The adsorption of PIB onto the surface of a water drop is investigated from the evolution of the interfacial tension over time, measured by the pendant drop method.[19,28] Figure 8 compares the results for a water drop in decane (M7) and a water drop in a very dilute PIB solution, made by adding 0.1 ml of M10 into roughly 120 ml of M7, resulting in a PIB concentration around 5 ppm. In both cases, the initial value

of $\sigma \approx 50$ dyn/cm agrees very well with the published value in the absence of a surfactant.[29,30] The low concentration PIB molecules in the bulk apparently have no effect on σ. In time, however, σ declines for both matrix liquids, and tends to limiting values in some 20 min. For the decane matrix, the roughly 12% reduction in σ indicates adsorption of contaminants pre-existing in the 99.9% pure decane (M7) as purchased from the vendor. For the added PIB, the reduction is greater at about 20%. The difference between the two data sets proves that PIB molecules indeed tend to adsorb onto water-decane interfaces, and that the adsorption reduces the interfacial energy.

Furthermore, we consider the time scale for the adsorption. Based on the Rouse-Zimm model for polymer chains in a dilute solution, Semenov and Joanny[25] calculated the adsorption time t_{ad} needed for an adsorption layer to reach equilibrium: $t_{ad} \sim t_a N^{2.24}$, where t_a is the monomer relaxation time and N the number of monomers in the chain. As the longest relaxation time of a Rouse chain is $\lambda \sim t_a N^2$,[21] and for our PIB molecules $N \sim 3.6 \times 10^4$, we arrive at $t_{ad} \sim \lambda N^{0.24} \sim 12.4$ ms as $\lambda \sim 1$ ms (Table I). The longer time scale in Fig. 8 must be due to diffusion of the polymer chains toward the drop surface. In film drainage, however, the diffusion time t_{di} will be much shorter because of the vastly reduced length scale. In fact, assuming $t_{di} \propto d^2$, d being the characteristic length for diffusion, the time scale of 20 min in Fig. 8 for a drop of diameter 3 mm implies a diffusion time of 1.3 μs for $d = 100$ nm in the thin film. Thus, t_{di} and t_{ad} are both much shorter than the rest time t_R, which is over 100 ms even for the smallest drops tested. Polymer adsorption, therefore, is completed quickly at the beginning of film drainage.

Finally, we estimate the maximum amount of polymer that can be adsorbed onto the drop. Typically, a polymer chain attaches to a surface by one or a few monomer sites. Thus, the chain dangles from the surface as strands or loops.[26,27] On the surface, an absorbed chain assumes a lateral dimension of $a N^{1/2}$, a being the monomer length.[27] The total number of chains inside the film is $n_c = \pi R_f^2 h \rho_2 c N_A / M_w$, where c is the weight-percent concentration of the PIB solution, and N_A is the Avogadro number. The total area these chains will occupy on the interface is therefore $a^2 N n_c$, which amounts to the following fraction of the drop area inside the film:

$$\eta = \frac{a^2 h c \rho_2 N_A}{m_w}, \tag{12}$$

where $m_w = 56$ is the molecular weight of the isobutylene monomer. Assuming $h = 100$ nm, $a = 0.4$ nm, we obtain $\eta = 0.628$ for a 0.5 wt. % PIB solution. Therefore, the adsorbed layer can hold more than all the polymer molecules in the thin film of 0.5 wt. % PIB solution. We have experimented with more concentrated PIB solutions in decane M7. The data are noisier because with higher polymer concentrations, the coalescence is complete instead of partial. To produce small primary drops within the same size range, we used micropipettes and found it difficult to control the release conditions. Nevertheless, the following trend is clear. The rest time of a water drop remains that for a polymer-free

matrix for a PIB concentration of 0.77 wt. %. For PIB concentration of 1 wt. % and higher, t_R starts to increase beyond that for a pure decane matrix, indicating saturation in surface adsorption. This saturation concentration is consistent with our estimation of η.

Based on the above, we conclude that the polymer chains in the film are cleared by adsorption within a short time at the beginning. Afterwards, the flow in the thinning film essentially involves the solvent alone. This explains the observations in Fig. 7. Since the flow in the film is largely simple shear, perhaps one should not have expected drastic viscoelastic effects in any event. Nevertheless, the absence of any effect by the polymers, not even through the shear viscosity, has come as a surprise.

We are aware of only one prior experiment on film drainage that involves polymer solutions. Dreher *et al.*[17] measured rest times of water drops on an organic/aqueous interface, where the organic matrix is made of various concentrations of PIB dissolved in a mixture of decane and PB. Despite the similar fluids, their data show no sign of polymer adsorption. For larger drops, the rest time t_R scales with the shear viscosity of the matrix. For drops smaller than a critical size ~ 1 mm, polymer in the matrix increases t_R beyond that expected from the elevated shear viscosity, and this augmentation is greater with higher PIB concentration.

A possible explanation for the lack of adsorption is that their solvent has 80% PB in decane, compared with 0% and 20% PB in our solvents (Fig. 7). Because of similar molecular structures, the attractive forces between PIB and PB molecules may help keep the PIB in the bulk. The higher solvent viscosity may also have played a role. For the anomalous increase in t_R for small drops, Dreher *et al.*[17] argued for the activation of elongational viscosity (strain-hardening). This is not convincing because the flow in the thinning film is mostly shear rather than extension.

To verify the effect of PB abundance, we have measured t_R using matrix fluids with 0% and 0.25 wt. % PIB in a solvent of 80% PB in decane M7. Between these two cases, the polymer lengthens t_R by 100% while increasing the shear viscosity by 20%. Thus, polymer adsorption is indeed inhibited by high concentration of PB. Moreover, the increase in t_R is beyond what can be accounted for by the shear viscosity. This confirms Dreher *et al.*'s observation, and may indicate that the polymer molecules have altered the microscopic conditions for the rupture of the film.

IV. EXPERIMENTAL RESULTS: PARTIAL COALESCENCE

While film drainage involves mostly shear flow, drop-interface coalescence features prominent extensional flow. Indeed, our results show that polymer in either the drop or the matrix phase strongly influences the partial coalescence cascade. In a recent Letter,[18] we have reported observations and analysis of partial coalescence when both components are Newtonian liquids. Although our focus here is on polymeric liquids, it seems necessary to briefly summarize the Newtonian findings as a starting point.

A. Newtonian liquids

High-speed video images suggest that the partial coalescence process consists of two stages: capillary wave propagation and filament pinch-off. After the rupture of the thinning film, the interface recedes rapidly to enlarge the conduit connecting the drop to the lower bulk. This sets off a capillary wave that propagates upward along the drop surface. By the time the wave front converges on the apex of the drop, the drop has been elongated into a liquid column, which becomes thinner as the drop fluid drains into the lower bulk. A neck forms at the base of the column and thins progressively as on a liquid filament, until a final pinch-off that produces the daughter drop.

The most revealing quantities are the coalescence time t_c, the interval from the film rupture to daughter drop pinch-off, and the drop size ratio ζ between the daughter and mother drops. Figure 9 plots t_c and ζ as functions of the Bond number Bo and the Ohnesorge number Oh. The coalescence time is nondimensionalized by the capillary time $\tau_c = (\bar{\rho} D^3 / \sigma)^{1/2}$. Note that the Bond number Bo increases with drop size D, while the Ohnesorge number Oh decreases with it. For the relatively low-viscosity fluids used here, we have identify three different regimes of partial coalescence with changing drop size. There exists an intermediate size range in which both Bo and Oh are small; the drop is too large for viscosity to be important yet too small for gravity to weigh in. Then t_c and ζ depend only on the density ratio, which does not vary much among the fluids (Table I). This is the self-similar inertio-capillary regime previously documented by Thoroddsen and Takehara,[14] where $t_c / \tau_c \approx 1$ and $\zeta \approx 0.5$ are more or less constant.

For larger drops, gravity becomes important and we identify a gravity regime where both t_c and ζ decrease with drop size. Taking into account the effects of gravity on propagation of interfacial waves and the downward velocity of the drop fluid at the neck, Chen *et al.*[18] developed scaling relations in terms of Bo that represent the data quite well. For smaller drops, on the other hand, a viscous regime prevails where both Oh and the viscosity ratio μ_* are important. Viscosity in either phase tends to delay the capillary instability and increase t_c. The effect on ζ is more complex since the longer t_c may be offset by a damped speed at which the drop fluid flows into the lower bulk. In general, ζ increases with increasing μ_*. Again, these effects may be formulated into scaling relations involving Oh and μ_*.[18]

Note the peculiar way data are plotted simultaneously against Oh and Bo. For each fluid pair, Bo·Oh⁴ is a constant and there is a unique correspondence between the two. Among different fluid pairs, however, there is no universal correspondence between Bo and Oh. Thus, in both figures we have plotted data against Bo in the gravitational and inertio-capillary regimes, and against Oh in the viscous regime.

Figure 9(b) clearly shows that partial coalescence occurs only for an intermediate range of drop diameters, outside which the coalescence is complete in one shot ($\zeta = 0$). Critical conditions can be identified from the right boundary of the gravity regime and the left boundary of the viscous re-
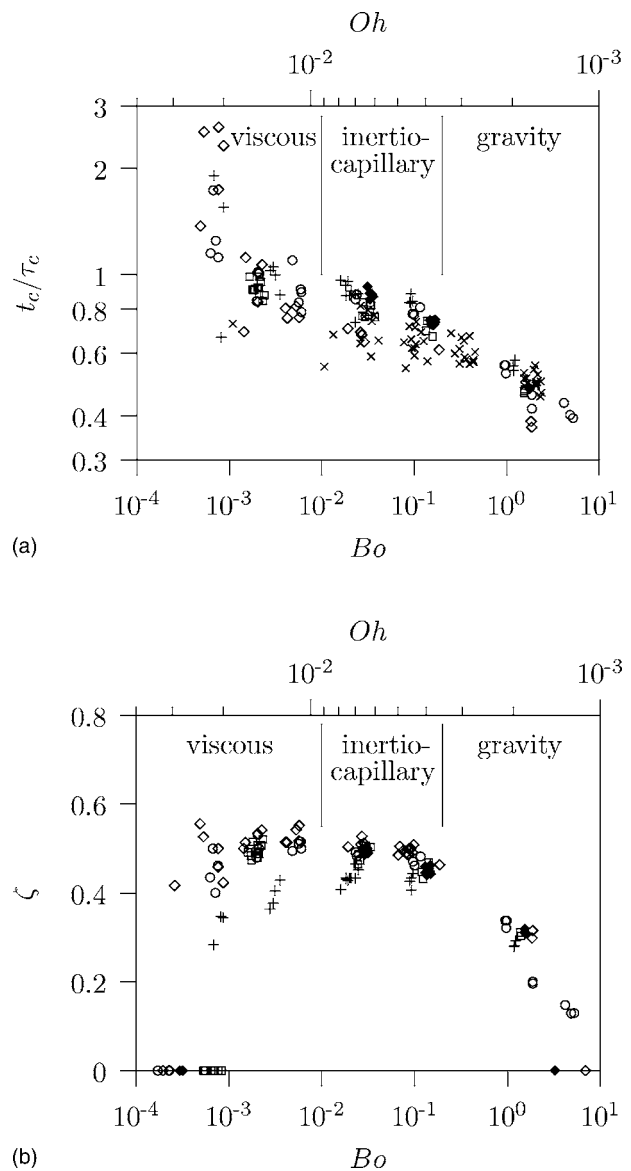

FIG. 9. Regimes of partial coalescence in Newtonian fluids. (a) Coalescence time scaled by the capillary time as a function of Bo and Oh. (b) The daughter-to-mother drop size ratio. The symbols are for D1/M7 (diamonds), D1/M8 (circles), D1/M9 (pluses), D2/M7 (squares), D3/M7 (filled diamonds), and ethanol in air (Ref. 14) (crosses). For each fluid pair, data are taken through the partial coalescence cascade as the drop diameter shrinks stepwise.

gime. For the fluids tested here, partial coalescence occurs for a range of D such that Bo $\lesssim 5$ and Oh $\lesssim 2 \times 10^{-2}$. For more viscous fluids, conceivably, the above picture will change. For instance, the self-similar inertio-capillary regime may be "squeezed out," and the criterion for partial coalescence may involve all the factors considered so far: inertia, gravity, capillarity, and viscosity.[15]

B. Non-Newtonian liquids

In contrast to the apparent absence of viscoelastic effects on the rest time, the partial coalescence cascade is greatly modified when polymer is added to either component. Figure 10 plots the coalescence time t_c and drop size ratio ζ as functions of the Bond number for three different fluid com-
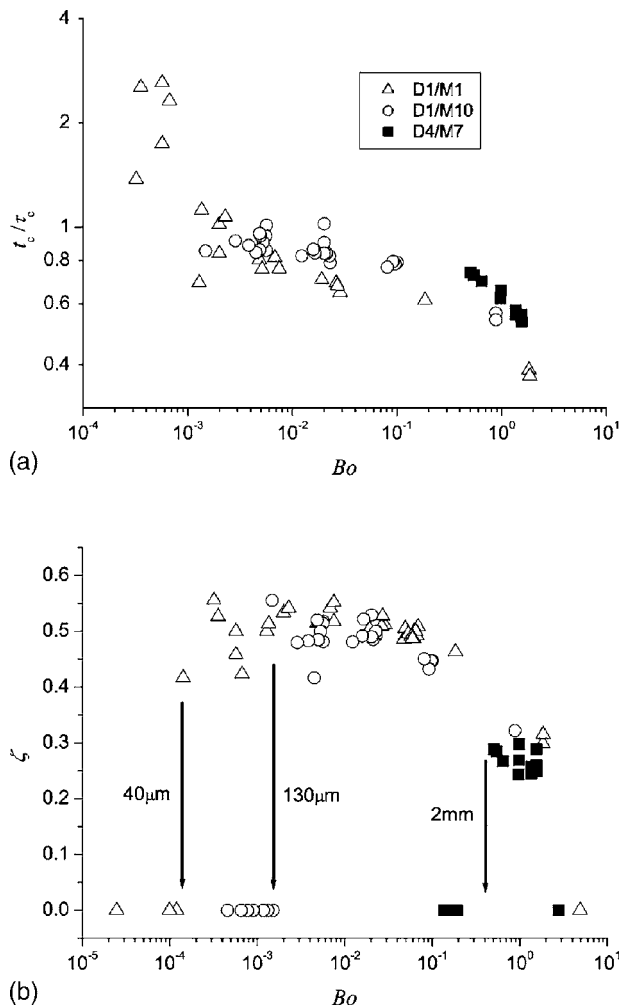
FIG. 10. Viscoelastic effects on partial coalescence. (a) Coalescence time; (b) drop size ratio. Symbols in (b) are the same as (a). The three vertical lines indicate the minimum drop sizes at which ζ plummets to zero.

binations. The baseline case is a water drop in the decane matrix (D1/M7). The other two cases have polymer solutions either in the drop (D4) or the matrix component (M10). Several related effects of viscoelasticity can be observed: (i) the coalescence time is increased; (ii) the drop size ratio is reduced; (iii) the minimum size for partial coalescence is increased. A direct consequence of (iii) is that partial coalescence is now limited to the large-drop regimes for the fluids tested. Judging from the behavior of t_c, we may say that the viscous regime is eliminated when the PIB solution M10 is the matrix. With the PEO solution D4 in the drop, both the viscous and the inertio-capillary regimes are gone and only the gravity regime remains. The upper bound for partial coalescence is lowered as well, though the change is not as prominent as that of the lower bound [Fig. 10(b)]. Between the two polymeric cases, viscoelasticity in the drop seems more potent in affecting both t_c and ζ than that in the matrix, especially considering that the PEO solution has a lower concentration and lower shear viscosity than the PIB solution (Table I). Other fluid combinations (D1/M5, D1/M6) have been tested, and show the same trend as described here.

To understand the flow mechanisms that produce the above effects, we have examined high-speed video footage of the partial coalescence cascade. Figure 11 shows snapshots of the last cycle of the cascade with the PEO solution D4 in the drop and decane in the matrix. After the film ruptures at $t=0$, a capillary wave propagates upward ($t=0.20$) and causes an uplifting at the top of the drop. The droplet at the base of the column is likely a matrix drop that is trapped during film rupture. Similar entrapment has been observed by Thoroddsen et al.[31] In time the liquid column thins and a neck forms due to capillary instability ($t=0.68$). Up to this stage, the process is very similar to partial coalescence in Newtonian fluids (cf. Fig. 4 in Chen et al.[18]), and the time elapsed at this point is close to the Newtonian value as well. But the viscoelasticity in the drop phase starts to be manifested as the neck thins further into a filament ($t=0.86$). Whereas the Newtonian filament pinches off at this stage, the viscoelastic filament persists and never breaks up. Thus partial coalescence is suppressed. Interestingly, the subsequent merging between the drop and the lower bulk is not a straightforward process. First, the drop falls under gravity ($t=1.08$) and "impacts" on the interface even though the filament still connects the two. A new episode of capillary wave propagation and filament necking ensues, leading to the formation of a thinner filament at $t=1.34$. In the next cycle, $t=1.40$ to $t=1.52$, the merging is finally complete. Thus, even though the filament never pinches off, the viscoelastic drop executes a "secondary-coalescence" cycle that mirrors the partial coalescence cascade. Each cycle is driven by the interchange among gravitational potential energy, interfacial energy and kinetic energy.

The longevity of the polymer filament is a well-known consequence of its high elongational viscosity. Previous theoretical and experimental studies[32–35] on capillary breakup of polymer filaments show that viscoelasticity increases the initial growth rate of disturbances but retards the eventual breakup. A characteristic "beads-on-a-string" morphology forms with generations of near-spherical drops connected by very thin threads. Because of the short time scale of coalescence, we did not observe beads-on-a-string in our experiment. Nevertheless, the thinning of the neck involves severe elongation of the polymeric liquid, and is therefore resisted by the tensile stress developed in the thread. To estimate the Deborah number, we take the velocity inside the filament to be the inertio-capillary velocity $v_f=(\sigma/\rho_1\epsilon)^{1/2}$, ϵ being the diameter of the filament which we take, rather generously, to be $D/10=0.12$ mm. Then the strain rate in the filament can be estimated as $v_f/\epsilon=3.95\times10^3$ s^{-1}. Even for the short relaxation time $\lambda=0.12$ ms for this solution (D4), the Deborah number reaches order 1 and viscoelastic strain-hardening is expected.

Thus, the suppression of capillary breakup explains how viscoelasticity in the drop arrests partial coalescence for smaller drops and raises the critical Bo value. For larger drops, filament pinch-off may take place but it will be delayed relative to the Newtonian case. This explains the longer coalescence time in Fig. 10(a). More fluid drains out of the drop during this time, thus reducing the drop size ratio ζ in Fig. 10(b). There are also fewer cycles of partial coalescence before complete merging.
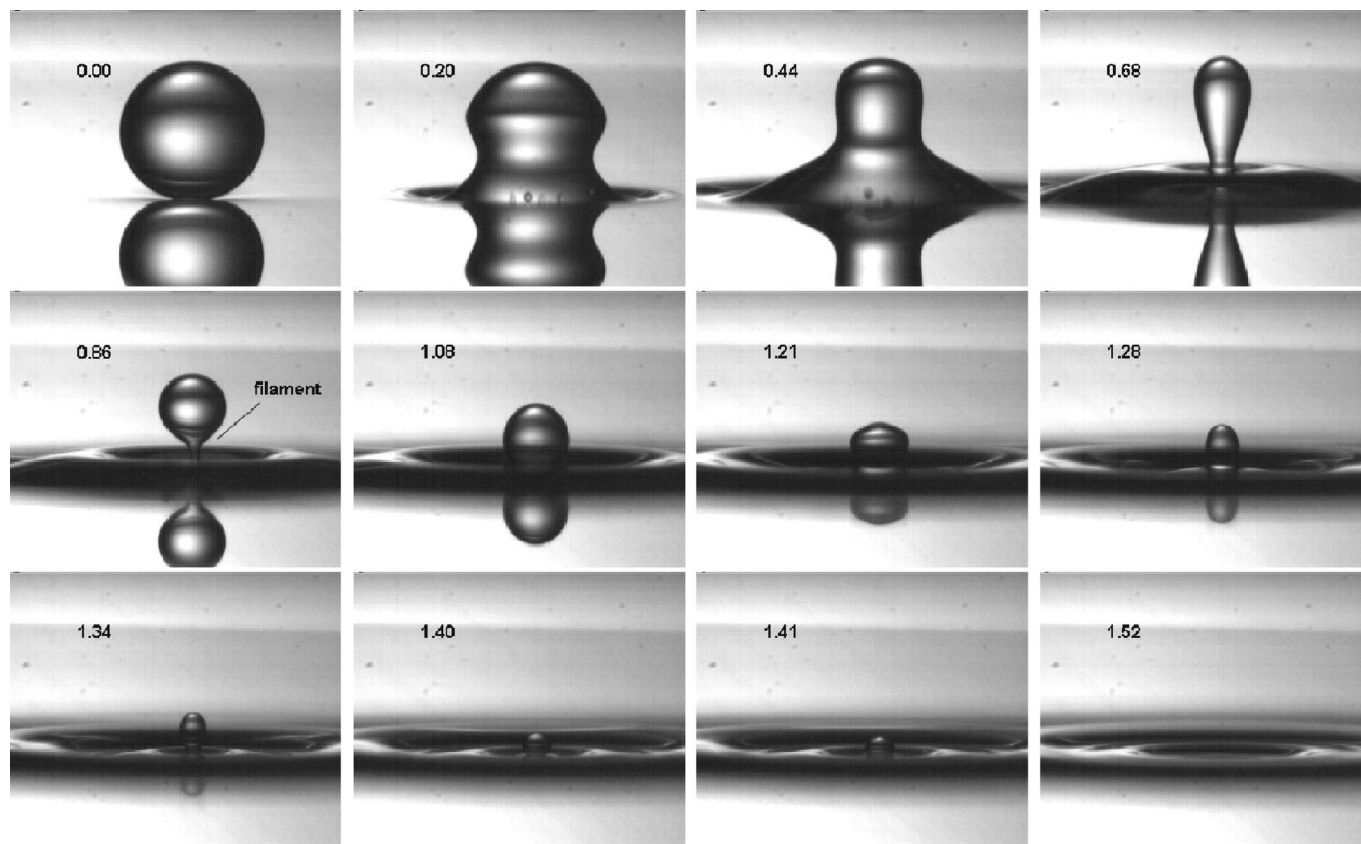
FIG. 11. Total coalescence for the last drop in the partial coalescence cascade. The drop phase is 0.18 wt. % PEO in water (D4), with drop diameter 1.2 mm and Bo=0.136. The matrix is decane (M7). The coalescence time is scaled by τ_c.

Viscoelasticity in the matrix has similar, albeit weaker, effects on partial coalescence, e.g., in lengthening the coalescence time t_c and reducing the drop size ratio ζ. In contrast to the voluminous literature on polymer fibers and jets breaking up in a Newtonian medium, there is little prior work on the inverse case of a Newtonian filament inside a polymeric matrix. Thus, we have carried out a set of experiments on pinch-off of pendant drops to explore this effect. A water drop is formed at the tip of a needle, at a flow rate of roughly

1 μl/s, in a matrix that is either pure decane (M7) or 0.5 wt. % PIB in decane (M10). The pendant drop falls under gravity and elongates the thread that hangs it from the needle. The final pinch-off is compared for the two matrix fluids in Fig. 12. Aside from the matrix composition, all conditions are the same for the two experiments.

The initial stages of neck formation and thinning are almost identical between the two cases. The moment $t=0$ corresponds to the pinch-off of the thread in the Newtonian
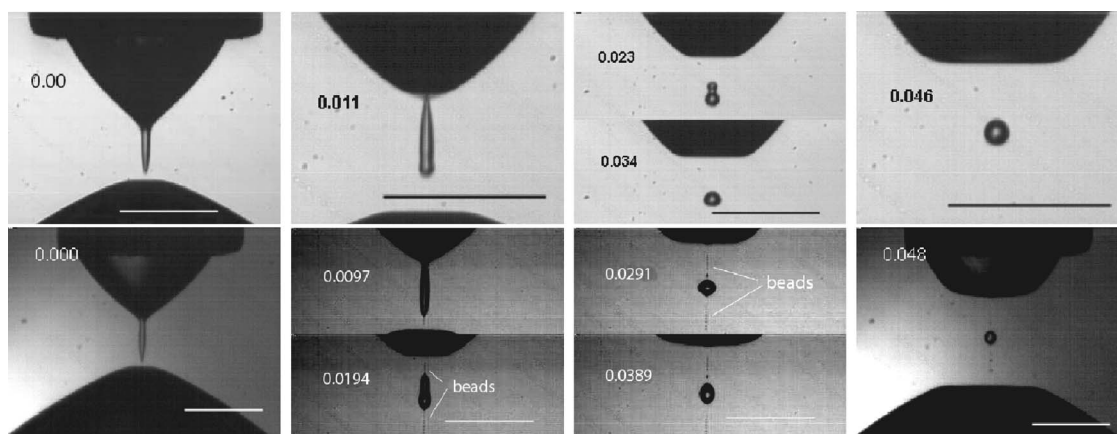

FIG. 12. Pinch-off of a pendant water drop in decane (M7, top row) and 0.5 wt. % PIB in decane (M10, bottom row). Three of the frames contain two pictures each. The length of the scale bar is 0.5 mm in all frames. The dimensionless time indicated in the pictures is scaled by $\tau_c = \sqrt{\bar{\rho}\delta^3/\sigma}$, $\bar{\rho}$ being the average density between the two fluids and $\delta=1.2$ mm being the needle's outer diameter. Its inner diameter is 0.84 mm.

decane matrix, at which time the thread has become exceedingly thin in the PIB matrix as well. In the decane matrix, the thread pinches off first at the base of the primary drop and then at the upstream location where the thread is attached to the fluid cone ($t=0.011$). The detached thread then retracts into a satellite drop ($t=0.023-0.046$). In the polymeric matrix, the thread does not pinch off at either location. Rather, the main mass of the thread contracts into a round drop that hangs in the middle of a very thin thread ($t=0.0194$). In time, smaller beads develop on the thread ($t=0.0291-0.0389$), creating the familiar beads-on-a-string morphology. The thread does not break up until much later. This is a well-known viscoelastic effect[35] distinct from the viscous effect noted by Doshi *et al.*[36] A detailed analysis of how viscoelasticity in the matrix suppresses capillary instability on a Newtonian filament is not yet available. Preliminary computations show that a large tensile stress develops in the matrix fluid surrounding the thinning filament. This stress resists further thinning of the filament, which would stretch the matrix fluid as well against the polymer stress. In our experiment, there is the further complication that the PIB chains in the matrix tend to adsorb onto the interface. Thus, the stretching of the adsorbed layer may have played a role as well. But the detailed micromechanisms are not explored in this work.

V. CONCLUSION

We have discussed a series of experiments on the coalescence between a drop and a liquid interface. Either of the drop and matrix phases can be Newtonian or viscoelastic, and we have focused on two features of the process: the rest time and the partial coalescence cascade. The results can be summarized as follows:

(*a*) *Rest time for Newtonian fluids*. With immobilized interfaces, film drainage consists of simple shear flow to leading order. The rest time scales linearly with the matrix viscosity, and increases with the drop diameter in a power law with an index of 2.15. This is similar to predictions of prior lubrication models, but there is no quantitative agreement with these models.

(*b*) *Rest time for polymer solutions*. At low concentrations, polymers in the matrix show no apparent effect on the rest time, as adsorption onto the interface clears the film of polymer chains. At higher polymer concentrations or with a "better" or more viscous solvent, some polymer chains remain in the film and raise the rest time.

(*c*) *Partial coalescence in Newtonian fluids*. Partial coalescence occurs for an intermediate range of drop sizes, and exhibits viscous, inertio-capillary and gravitational regimes for low-viscosity fluids. Partial coalescence hinges on the pinch-off of the daughter drop by capillary instability, and is inhibited by viscosity for drops that are too small, and by gravity for those too large.

(*d*) *Partial coalescence in polymer solutions*. Polymers in either the drop or the matrix phase tend to increase the coalescence time, reduce the drop-size ratio, and elevate the minimum drop size for partial coalescence. The effect is stronger when the viscoelasticity is in the drop phase than

the matrix phase. The mechanism seems related to the suppression by viscoelasticity of capillary instability on a thin thread.

We must emphasize that this work has left several questions unanswered. Foremost is the role of surfactants in the process. We have not added surfactants intentionally but stray surfactants have played important parts in immobilizing the interface and possibly modifying the final stage of film thinning. Similar indications have come from other researchers.[37] Future investigations that carefully control and monitor the concentration and distribution of surfactants during drop-interface coalescence will help clarify this picture. A somewhat related question is the process of polymer adsorption. While thermodynamic theories have been built for the kinetics of adsorption and desorption,[27] the fluid-mechanical implications have not been explored at any length. Possibly, disturbance of the adsorbed layer will introduce complex surface rheology into the process of interfacial rupture and coalescence. In this work, the complication of polymer adsorption has prevented the construction of a clear-cut picture for the effect of bulk rheology on film drainage. Finally, we still do not have a detailed understanding of how the capillary instability on a filament is affected by viscoelasticity in the surrounding medium.

APPENDIX: INTERFACIAL IMMOBILIZATION

Earlier theoretical studies on film drainage, e.g., Charles and Mason,[2] assumed immobile interfaces as a matter of necessity, because this greatly simplifies lubrication analysis by excluding the inside of the drop from consideration. More sophisticated models have allowed the possibility of interfacial slip and indeed highlighted the role of the eddies inside the drop.[7,9] In reality, the interface may be immobilized, at least partially, by two factors: high viscosity of the drop phase and a Marangoni stress due to surfactants, either intentionally added or naturally occurring as contaminants. As the shear flow near the interface causes nonuniform distribution of surfactants, a gradient of the interfacial tension amounts to a tangential stress that resists the shear motion. In our experiments, we have added no surfactants and have attempted to remove contaminants from the fluids by filtration. But evidence indicates that stray surfactants have acted to immobilize the interface.

A simple lubrication analysis shows that the interface will be immobilized by a minute amount of surfactant. Consider the axisymmetric film between the drop and the interface. We denote the film thickness by $h(r)$, where r is the radial coordinate originating from the center of the film, and

the vertical coordinate is z. More general lubrication analysis has been done in the past to determine h.[38] But our goal is more limited, and we will write out only the equations needed for our argument instead of the complete set.

Using the standard lubrication assumption within the film, one obtains a parabolic velocity profile for the radial flow

$$u(z) = v - \frac{h\partial_r p}{2\mu_2}\left(z - \frac{z^2}{h}\right), \tag{A1}$$

where v is the slip velocity on the interfaces, $\partial_r p = \partial p/\partial r$ is the radial pressure gradient, and μ_2 is the viscosity of the fluid in the film. A balance of tangential stresses on the drop surface requires

$$\mu_2 \partial_z u = -\frac{\mu_1 v}{R} + \partial_r \sigma(r) \quad \text{at } z = h, \tag{A2}$$

where μ_1 is the drop phase viscosity, and the first term on the right-hand side is an estimation of the shear stress inside the drop surface. The second term is the gradient of the interfacial tension σ, which is assumed to depend on the surfactant concentration $c(r)$ linearly

$$\sigma = \sigma_0 - kc, \tag{A3}$$

where σ_0 is the interfacial tension of a clean interface, and the coefficient k depends on the surfactant and temperature.[39] We further assume that the surfactant is insoluble in either bulk fluid, and its distribution on the interface is determined by convection and diffusion

$$vc = D_s \partial_r c, \tag{A4}$$

where D_s is the surface diffusivity of the surfactant. Note that we have assumed a quasistatic situation and neglected temporal derivatives. Substituting Eqs. (A1), (A3), and (A4) into the boundary condition Eq. (A2) leads to an expression for the slip velocity

$$v = \frac{hR(-\partial_r p)}{2(\mu_1 + \mu_s)}, \tag{A5}$$

where the "interfacial viscosity" $\mu_s = kRc/D_s$. This equation is similar to the classic results of Levich[40] on the slip velocity on a drop falling through a surfactant solution. The interfacial mobility can be represented by the magnitude of v compared to, say, the difference between the centerline and slip velocities

$$\beta = \frac{v}{u(h/2) - v} = \frac{4R}{h}\frac{\mu_2}{\mu_1 + \mu_s}. \tag{A6}$$

The interface is immobilized when β falls much below unity. As intuitively anticipated, the drop viscosity and Marangoni stress both tend to suppress interfacial mobility while the matrix phase viscosity tends to promote it. β also depends on the drop-diameter to film-thickness ratio. As the film grows thinner, interfacial slip may become substantial even if it was inhibited earlier. Note that β is independent of the driving pressure gradient (or the buoyant weight of the drop).

To make an order-of-magnitude estimation of β, we need the surfactant-related parameters in μ_s. In our experiments, no quantitative knowledge is available on the contaminants acting as surfactants. We circumvent this difficulty by recognizing that kc reflects the decrease in σ from that of the clean interface σ_0, and cannot exceed the latter. For a water-decane interface, $\sigma_0 = 50$ dyn/cm (cf. Fig. 8). But we will conservatively assume that the surfactant concentration is low and can cause only a change of 1% of σ_0. Then for droplets of 1 mm diameter and an estimate of $D_s \sim 10^{-5}$ cm^2/s,[40] we get $\mu_s \sim 250$ Pa s. Comparing this with the values of $\mu_1 \sim \mu_2 \sim 10^{-3}$ Pa s shows that μ_1 can be ignored with respect to μ_s, and further that $\beta \sim 1.6 \times 10^{-5} R/h$. Thus, interfacial slip can be ignored as long as $h \gg 8$ nm, which is much below the critical film thickness $h \sim 100$ nm required for van der Waals forces or other short-range forces to cause film rupture.[12] Thus we are led to conclude that the smallest amount of surfactants will immobilize the interface completely.

As a separate test of interfacial slip, we measured the terminal settling velocity of water droplets through a viscous matrix (M8). Results show that the droplets obey the Stokes law, not the Rybczyński-Hadamard law.[40] For example, for a droplet of diameter 1.24 mm, the Stokes law predicts a fall velocity of 10.0 cm/s, while the Rybczyński-Hadamard law predicts 12.9 cm/s. The measured value is 9.60 cm/s. For droplets of similar sizes, the Bond number is very small and the droplets do not deviate from the spherical shape.

[1]G. E. Charles and S. G. Mason, "The coalescence of liquid drops with flat liquid/liquid interfaces," J. Colloid Sci. **15**, 236 (1960).

[2]G. E. Charles and S. G. Mason, "The mechanism of partial coalescence of liquid drops at liquid/liquid interfaces," J. Colloid Sci. **15**, 105 (1960).

[3]B. K. Chi and L. G. Leal, "A theoretical study of the motion of a viscous drop toward a fluid interface at low Reynolds number," J. Fluid Mech. **201**, 123 (1989).

[4]X. Zheng, J. Lowengrub, A. Anderson, and V. Cristini, "Adaptive unstructured volume remeshing—II: Application to two- and three-dimensional level-set simulations of multiphase flow," J. Comput. Phys. **208**, 626 (2005).

[5]J.-D. Chen, P. S. Hahn, and J. C. Slattery, "Coalescence time for a small drop or bubble at a fluid-fluid interface," AIChE J. **30**, 622 (1984).

[6]A. F. Jones and S. D. R. Wilson, "The film drainage problem in droplet coalescence," J. Fluid Mech. **87**, 263 (1987).

[7]S. G. Yiantsios and R. H. Davis, "On the buoyancy-driven motion of a drop towards a rigid surface of a deformable interface," J. Fluid Mech. **217**, 547 (1990).

[8]A. Bhakta and E. Ruckenstein, "Decay of standing foams: drainage, coalescence and collapse," Adv. Colloid Interface Sci. **70**, 1 (1997).

[9]G. V. Jeffreys and J. L. Hawksley, "Coalescence of liquid droplets in two-component two-phase systems: Part II. theoretical analysis of coalescence rate," AIChE J. **11**, 418 (1965).

[10]T. D. Hodgson and D. R. Woods, "The effect of surfactants on the coalescence of a drop at an interface," J. Colloid Interface Sci. **30**, 429 (1969).

[11]S. A. K. Jeelani and S. Hartland, "Effect of interfacial mobility on thin film drainage," J. Colloid Interface Sci. **164**, 296 (1994).

[12]G. D. M. MacKay and S. G. Mason, "The gravity approach and coalescence of fluid drops at liquid interfaces," Can. J. Chem. Eng. **41**, 203 (1963).

[13]A. D. Nikolov and D. T. Wasan, "Effects of surfactant on multiple stepwise coalescence of single drops at liquid-liquid interfaces," Ind. Eng. Chem. Res. **34**, 3653 (1995).

[14]S. T. Thoroddsen and K. Takehara, "The coalescence cascade of a drop," Phys. Fluids **12**, 1265 (2000).

[15]Z. Mohamed-Kassim and E. K. Longmire, "Drop coalescence through a liquid/liquid interface," Phys. Fluids **16**, 2170 (2004).

[16]F. Blanchette and T. P. Bigioni, "Partial coalescence of drops at liquid interfaces," Nat. Phys. **2**, 254 (2006).

[17]T. M. Dreher, J. Glass, A. J. O'Connor, and G. W. Stevens, "Effect of rheology on coalescence rates and emulsion stability," AIChE J. 45, 1182 (1999).

[18]X. Chen, S. Mandre, and J. J. Feng, "Partial coalescence between a drop and a liquid-liquid interface," Phys. Fluids 18, 051705 (2006).

[19]S. H. Anastasiadis, J.-K. Chen, J. T. Koberstein, A. F. Siegel, J. E. Sohn, and J. A. Emerson, "The determination of interfacial tension by video image processing of pendant fluid drops," J. Colloid Interface Sci. 119, 55 (1987).

[20]L. E. Rodd, T. P. Scott, D. V. Boger, J. J. Cooper-White, and G. H. McKinley, "The inertio-elastic planar entry flow of low-viscosity elastic fluids in micro-fabricated geometries," J. Non-Newtonian Fluid Mech. 129, 1 (2005).

[21]R. B. Bird, C. F. Curtiss, R. C. Armstrong, and O. Hassager, *Dynamics of Polymeric Liquids* (Wiley, New York, 1987), Vol. 2.

[22]P. Ghosh and V. A. Juvekar, "Analysis of the drop rest phenomenon," Trans. IChemE, Part C 80, 715 (2002).

[23]D. R. Woods and K. A. Burrill, "The stability of emulsions," J. Electroanal. Chem. Interfacial Electrochem. 37, 191 (1972).

[24]P. G. de Gennes, "Polymer solutions near an interface. 1. Adsorption and depletion layers," Macromolecules 14, 1637 (1981).

[25]A. N. Semenov and J.-F. Joanny, "Kinetics of adsorption of linear homopolymers onto flat surfaces: Rouse dynamics," J. Phys. II 5, 859 (1995).

[26]D. Myers, *Surfaces, Interfaces, and Colloids: Principles and Applications*, 2nd ed. (Wiley, New York, 1999).

[27]B. O'Shaughnessy and D. Vavylonis, "Non-equilibrium in adsorbed polymer layers," J. Phys.: Condens. Matter 17, R63 (2005).

[28]R.-J. Roe, V. L. Bacchetta, and P. M. G. Wong, "Refinement of pendent drop method for the measurement of surface tension of viscous liquid," J. Phys. Chem. 71, 4190 (1967).

[29]M. Mulqueen and D. Blankschtein, "Theoretical and experimental investigation of the equilibrium oil-water interfacial tensions of solutions containing surfactant mixtures," Langmuir 18, 365 (2002).

[30]S. A. Nespolo, D. Y. C. Chan, F. Grieser, P. G. Hartley, and G. W. Stevens, "Forces between a rigid probe particle and a liquid interface: Comparison between experiment and theory," Langmuir 19, 2124 (2003).

[31]S. T. Thoroddsen, T. G. Etoh, and K. Takehara, "Air entrapment under an impacting drop," J. Fluid Mech. 478, 125 (2003).

[32]M. Goldin, J. Yerushalmi, R. Pfeffer, and R. Shinnar, "Breakup of a laminar capillary jet of a viscoelastic fluid," J. Fluid Mech. 38, 689 (1969).

[33]Y. Christanti and L. M. Walker, "Surface tension driven jet break up of strain-hardening polymer solutions," J. Non-Newtonian Fluid Mech. 100, 9 (2001).

[34]J. Li and M. A. Fontelos, "Drop dynamics on the beads-on-string structure for viscoelastic jets: A numerical study," Phys. Fluids 15, 922 (2003).

[35]M. S. N. Oliveira and G. H. McKinley, "Iterated stretching and multiple beads-on-a-string phenomena in dilute solutions of highly extensible flexible polymers," Phys. Fluids 17, 071704 (2005).

[36]P. Doshi, I. Cohen, W. W. Zhang, M. Siegel, P. Howell, O. A. Basaran, and S. R. Nagel, "Persistence of memory in drop breakup: The breakdown of universality," Science 302, 1185 (2003).

[37]R. V. Craster, O. Matar, and D. T. Papageorgiou, "Pinchoff and satellite formation in surfactant covered viscous threads," Phys. Fluids 14, 1364 (2002).

[38]L. Y. Yeo, O. K. Matar, E. S. P. de Ortiz, and G. H. Hewitt, "Film drainage between two surfactant-coated drops colliding at constant approach velocity," J. Colloid Interface Sci. 257, 93 (2003).

[39]A. W. Adamson, *Physical Chemistry of Surfaces*, 3rd ed. (Wiley, New York, 1976).

[40]V. Levich, *Physicochemical Hydrodynamics* (Prentice-Hall, Englewood Cliffs, 1962).